International Research Journal of Engineering and Technology (IRJET) e-ISSN: 2395 -0056
Volume: 02 Issue: 06 | Sep-2015 www.irjet.net p-ISSN: 2395-0072

SOLAR POWERED REACTIVE POWER COMPENSATION IN SINGLE-PHASE OPERATION OF MICROGRID

B.Praveena[1], S.Sravanthi[2]

[1]PG Scholar, Department of EEE, JNTU Anantapur, Andhra Pradesh, India
[2] PG Scholar, Department of EEE, JNTU Anantapur, Andhra Pradesh, India

ABSTRACT: A new coordinated control of distributed generators and distributed static compensator (DSTATCOM) is presented in this project. Microgrids are combination of many renewable resources connected together. The voltage limit may change due to the high penetration of the renewable resources. So the reactive power control is not always possible to achieve with optimum location and three-phase supply. A communication based single-phase control of DSTATCOM is presented. The power flow in the line is also controlled in this project. The Power flow and voltage at different locations are communicated with the DSTATCOM to modulate the reactive compensation. The single phase DSTATCOM compensates the reactive power deficiency in the phase when DG supplies the maximum available active power. A primary control measures the DSTATCOM ensures the part of reactive power in case of communication failure. The control method is extended to test the system with real model of solar panel and results are discussed.

Keywords: Distributed generators (DG), Photovoltaic (PV), Distribution Static Compensator (DSTATCOM).

1. INTRODUCTION

Systematic coordinated control of DGs and DSTATCOM done in single-phase operation of microgrid [1]. Microgrid formation involving Distributed generators benefits the consumers and power utilities with local power generation [2]. Distributed generation refers to power generation at the point of consumption generating power on-site, rather than centrally, eliminates the cost, complexity, interdependencies, inefficiencies associated with transmission and distribution. Although feeders' capacity increased with the help of suitable DG, improvement of power quality or system reliability is not inevitable [3]. Assumption that DGs alone enhances the reliability of the system cannot be done and further demand rises for effort to secure system reliability. Main measure among many is the collaborated regulation of DGs and compensation devices. Alleviation of power quality circumstances can be accomplished by keeping under systematic review and recompense through power electronic devices in present time microgrids [4]. High usage of DGs results in voltage drop which is one among the contentious challenges in a microgrid and Voltage drop acceptable limit is 10% [5]. Pressing case about power quality arises due to usage of multi micro-sources [6]. Problem of voltage regulation prevails at feeders' end which necessitates the improvised collaboration of DGs with DSTATCOM to avoid the case of voltage falling below the acceptable value. Voltage control and load sharing are done by parallel DGs operations. DSTATCOM equips entailed voltage support and power quality improvement. DSTATCOM is helpful in elimination of harmonics, provision of load balance, improvisation of supply power factor and load terminal voltage at point of common coupling. Either in voltage control mode or current control mode DSTATCOM can be operated. For the purpose of feedback signals in PI controllers DSTATCOM dc bus voltage is used. DSTATCOM compels distribution bus voltage as sinusoids of balanced type in voltage control mode where as in current control mode cancellation of distortion due to loads can be done. Operation of DGs with voltage control and to accomplish reactive power collaboration with DGs is worth having DSTATCOM in voltage control. Every time with three-phase devices it is not possible to result compensation of reactive power with feeders spread out apart by three-phase devices. Hence, with single phase devices it is reliable to accomplish reactive power compensation. DSTATCOM gives faster response independent of network impedance, modular, can be interfaced with real power sources, superior performance compared to some other compensating devices. Photovoltaic (PV) is the name of a method of converting solar energy into direct current electricity using semiconducting materials that exhibit the photovoltaic effect, a phenomenon commonly studied in

subjects physics, photochemistry and electrochemistry. Photovoltaic is a renewable resource of electricity which uses the sunlight as a source of power generation which is advantageous to use compared to some other non-renewable resources Photovoltaic array is the complete power-generating unit consisting of any number of PV modules and panels. Photovoltaic is helpful in electrical energy production in a reliable and eco-friendly manner.

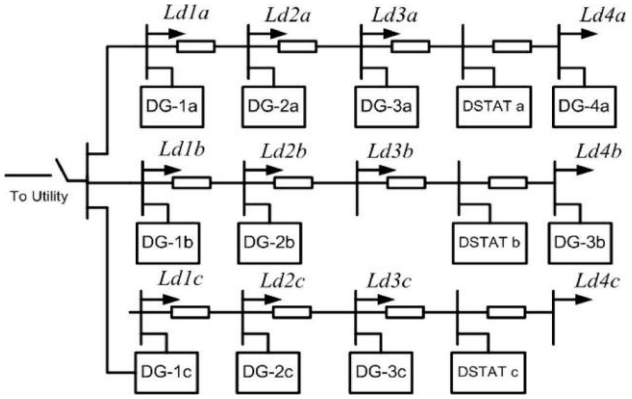

Fig.1 System under consideration.

2. STRUCTURE OF MICROGRID SYSTEM

Fig. 1 shows the microgrid system structure under consideration with three feeder sections of DGs and loads connected. DGs represented by DG1a, DG2a, DG3a, DG4a, DG1b, DG2b, DG3b, DG1c, DG2c, DG3c which means DGs first, second, third, fourth connected to corresponding phases a, b, c. Assumption of DGs as VSC interfaced is made. DGs supply maximum available power and utility supplies extra power required by loads in grid-connected mode. DGs supply total power demanded in islanded mode. Assumption of islanded mode power demand more than DGs total power output and to meet power balance loads shedded partly. Ld1a, Ld2a, Ld3a, Ld4a, Ld1b, Ld2b, Ld3b, Ld4b, Ld1c, Ld2c, Ld3c, Ld4c represents loads. DSTAT a, DSTAT b, DSTAT c indicates DSTATCOM locations. Feeder impedance not neglected. Parameters of system and DG ratings given in table format I-IV

TABLE I

GRID AND LOAD IN THE MICROGRID

Grid	
Voltage	400 V L-L RMS
Frequency	50Hz
Line Impedance	R=0.1 Ω, L=0.001 H
Load Type	
Resistive	Single-Phase Resistive load

TABLE II

CONVERTER AND CONTROLLER

No. of Converter in Phase A	4
No. of Converter in Phase B	3
No. of Converter in Phase C	3

Rated output power of DGs	Phase A	phase B	phase C
DG-1	1.5KW	4.0KW	5.0KW
DG-2	4.0KW	4.0KW	4.0KW
DG-3	5.0KW	3.0KW	5.0KW
DG-4	5.0KW	xx	xx

Converter Structure	Single-phase H-Bridge Inverter
Converter Loss	R=0.1 Ω per phase
Transformer	0.400/0.230 KV, 0.5MVA, Ltr=4.4mH
LC Filter	Lf=49.8 mH , Cf=50 μF

TABLE III

DG CONTROLLER GAINS

Power Controller Proportional Gain Kp	0.001
Power Controller Integral Gain Tn	0.01
Reactive Power Controller Proportional Gain Kq	0.0013
Reactive Power Controller Integral Gain Tn	0.011
d Axis Current Controller Proportional Gain Kid	2
d Axis Current Controller Integral Gain Tn	0.01
q Axis Current Controller Proportional Gain Kid	2
q Axis Current Controller Integral Gain Tn	0.012
Voltage Controller Gain m1	0.016V/VAr

TABLE IV

DSTATCOM CONTROLLER GAINS

Power Controller Proportional Gain Kps	0.0013
Power Controller Integral Gain Tn	0.012
Reactive Power Controller Proportional Gain Kqs	0.0034
Reactive Power Controller Integral Gain Tns	0.04
d Axis Current Controller Proportional Gain Kid	2.5
d Axis Current Controller Integral Gain Tn	0.016
q Axis Current Controller Proportional Gain Kid	3.3
q Axis Current Controller Integral Gain Tn	0.027
Voltage Controller Gain m1	0.012V/VAr

Depending upon power flow and voltage in the line reactive compensation regulated. Due to frequent load switching and DG power output variations, feeders' real and reactive power flow changes as a result voltage changes. For accomplishment of voltage profile quick control, it is profitable to take power flow into account in DSTATCOM control.

Assumptions made are as follows:

- Depending upon converter safe operating area, DGs inject maximum available power in microgrid and reactive current limit derived from maximum current rating and d axis active current limits the reactive power generation.
- According to DGs ratings in islanded mode reactive power shared by them in the time of low reactive power demand.
- Reactive power generated by DSTATCOM during DG reaches reactive power limit and DG bus voltage goes below voltage regulation limit.
- Reactive power capability increased by lowering the active power generation within limit When a DG with reactive power limit stays for 5 cycles.
- Generated or absorbed reactive power by DSTATCOM limited based on converter circuit parameter and maximum rating.

3. FORMULATION OF CONTROL PRINCIPLES FOR DG AND DSTATCOM

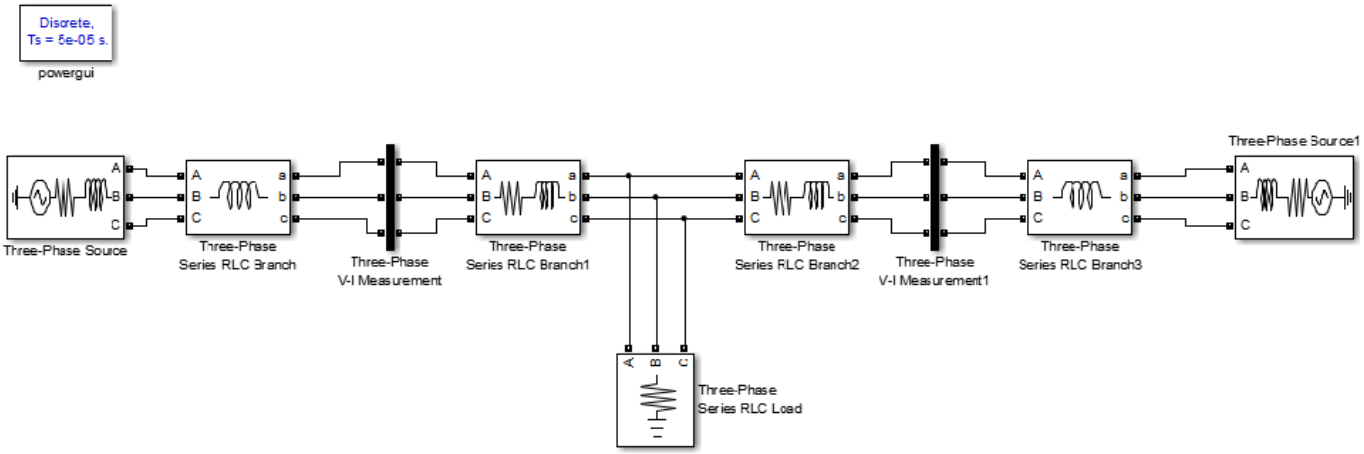

Fig.2 Two machine system

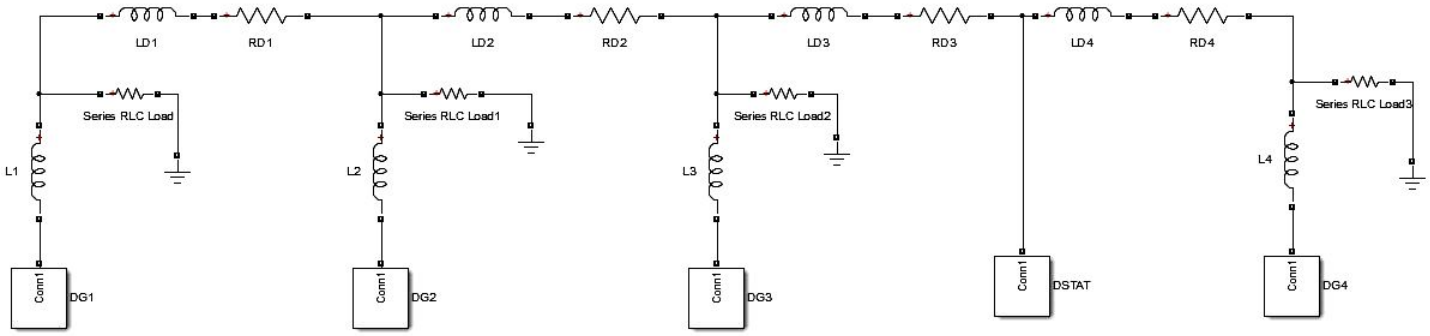

Fig.3 Multi machine system

Fig. 2 shows the two machine system of 2 DGs connected in 2 buses and a load and Fig 3. shows the multi machine system of 4 DGs connected in 4 buses and DSTAT connected at Bus DSTAT. Both two machine and multi machine configurations are used in formulating the control principle for the DGs and DSTATCOM. Consideration of grid connected and islanded mode operations done.

Assumption of P_{reflim} and Q_{reflim} as DG-1 maximum available active and reactive power and DG-1 converter voltage reference regulated with droop control in islanded mode and calculated as V_{1mag}

$$V_{1ref} = V_{1mag} - m_1 Q_1 \quad \rightarrow(1)$$

Q_1 limited to maximum reactive power value $Q_{1max.}$

For Fig. 2, Bus 1 power flow is as follows

$$P_1 = \eta[R_{D1}(V_{11} - V\cos(\delta_{11} - \delta)) + X_{D1} V \sin(\delta_{11} - \delta)]$$

$$Q_1 = \eta[-R_{D1} V \sin(\delta_{11} - \delta) + X_{D1}(V_{11} - V\cos(\delta_{11} - \delta))]$$

$$\eta = V_{11}/(R_{D1}^2 + X_{D1}^2)$$

$$X_{D1} P_1 - R_{D1} Q_1 = V_{11} V \sin(\delta_{11} - \delta) \quad \rightarrow(2)$$

$$R_{D1} P_1 + X_{D1} Q_1 = V_{11}^2 - V V_{11} \cos(\delta_{11} - \delta) \quad \rightarrow(3)$$

Linearization of (2) and (3) over nominal values of V_{110} and δ_{110} then

$$X_{D1}\Delta P_1 - R_{D1}\Delta Q_1 = (V_{110} V)(\Delta\delta_{11} - \Delta\delta) + (\delta_{110} V)\Delta V_{11} \rightarrow(4)$$

$$R_{D1}\Delta P_1 + X_{D1}\Delta Q_1 = (2V_{110} - V)\Delta V_{11} \quad \rightarrow(5)$$

Output voltage of DG-1 is

$$\begin{bmatrix}\delta_{11} - \Delta\delta \\ \Delta V_{11}\end{bmatrix} = K(V) \begin{bmatrix}\frac{X_{F1}}{Z_1} & -\frac{R_{F1}}{Z_1} \\ \frac{X_{F1}}{Z_1} & \frac{R_{F1}}{Z_1}\end{bmatrix} \begin{bmatrix}\Delta P1 \\ \Delta Q1\end{bmatrix} = K(V) T \begin{bmatrix}\Delta P1 \\ \Delta Q1\end{bmatrix} \rightarrow(6)$$

$$Z_1 = \sqrt{R_{D1}^2 + X_{D1}^2}$$

$$K(V) = Z_1 \begin{bmatrix}V_{110} V & \delta_{110} V \\ 0 & 2V_{110} - V\end{bmatrix}^{-1}$$

Linearizing (4) over nominal voltage V_0 then

$$R_{D1}\Delta P_1 + X_{D1}\Delta Q_1 = -V_{11} V_0 \Delta V$$

$$\Delta V = -\frac{R_{D1}\Delta P_1 + X_{D1}\Delta Q_1}{V_{11} V_0} \quad \rightarrow(7)$$

DSTATCOM voltage reference in two machine system is

$$V_{statref} = V_0 - m_{STAT} Q_{STAT} + K_1 \frac{R_{D1}\Delta P_1 + X_{D1}\Delta Q_1}{V_{11} V_0} + K_2 \frac{R_{D2}\Delta P_2 + X_{D2}\Delta Q_2}{V_{22} V_0}$$

$$\rightarrow(8)$$

$Q_{STATLIM}$ is DSTATCOM capacity that limits the Q_{STAT}

Gains- m_{STAT}, K_1, K_2

DSTATCOM voltage reference in multi machine system is

$$V_{statref} = V_0 - m_{STAT} Q_{STAT} + K_1 \frac{R_{D1} P_1 + X_{D1} Q_1}{V_{11} V_{22}} + K_2 \frac{R_{D2} P_2 + X_{D2} Q_2}{V_{22} V_{33}} + K_3 \frac{R_{D3} P_3 + X_{D3} Q_3}{V_{33} V_{stat}} + K_4 \frac{R_{D4} P_4 + X_{D4} Q_4}{V_{44} V_{stat}}$$

→(9)

$$P_{1ref} = P_{1maxavail} - lim[0, 0.05pu, k_{pr}(V_{110} - V_{11})]$$

$$if\ (V_{110} > V_{11})$$ →(10)

Reactive current reference is

$$i_{reactivelim} = \sqrt{(i_{max}^2 + i_d^2)}$$ →(11)

i_{max} is maximum converter current rating, i_d is d axis converter current.

4. CONVERTER CONTROL FOR DGS AND DSTATCOM

Technique of dq transformation for single phase is implemented for transformation of voltage and current in DG and DSTATCOM.

$$V(t) = V_m \sin(\omega t - \varphi)$$

$$V(t) = V_d \sin(\omega t) - V_q \sin(\omega t)$$

$$V_d(t) = V_m \cos(\varphi) \text{ and } V_q(t) = V_m \sin(\varphi)$$

DG: The structure and control for all the DG converters are similar. Here, only structure and control of DG-1 converter are described. Converter structure of DG-1 is as shown in Fig. 4. Single-phase converter consists of 4 IGBT switches output voltage of ac side connected to output filter capacitor through transformer. Converter control scheme of DG-1 is shown in Fig. 5.

DSTATCOM: DSTATCOM converter structure is shown in Fig. 10. DC side capacitor connected to H-Bridge and ac side voltage e_{STAT} connected to output filter capacitor through transformer. Converter structure of DSTATCOM is shown in Fig. 6. Converter control scheme of DSTATCOM is shown in Fig. 7. Equation (9) is used for the calculation of DSTATCOM output voltage reference.

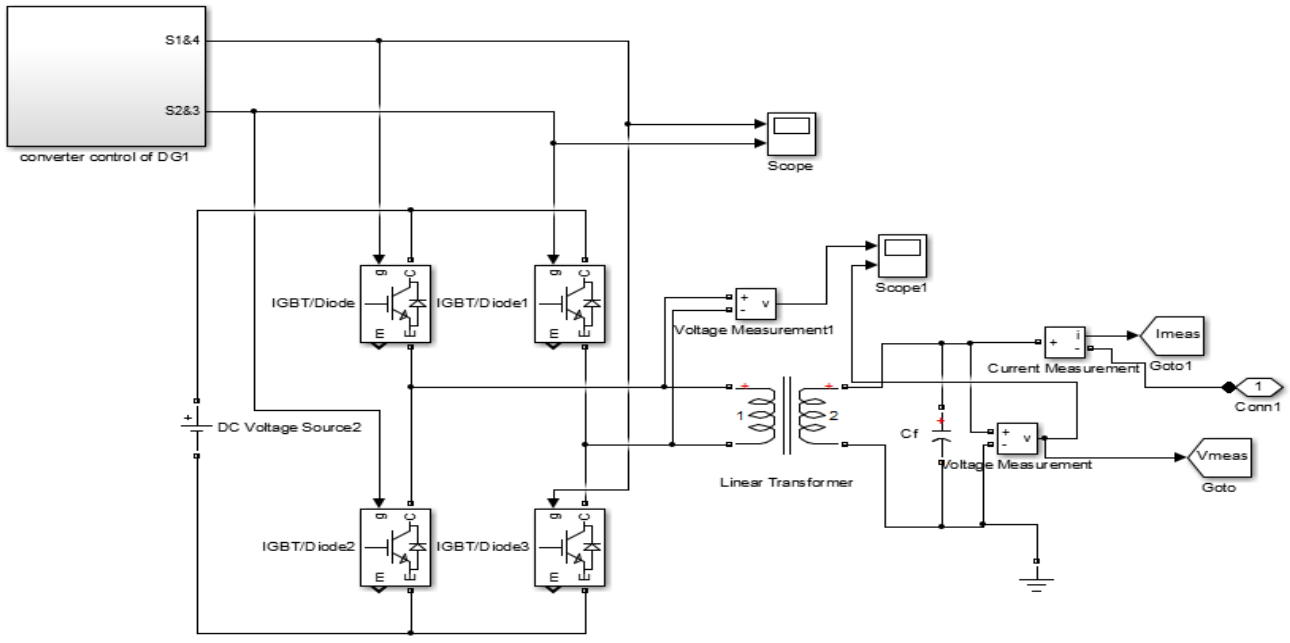

Fig.4a Converter structure of DG-1 without PV array

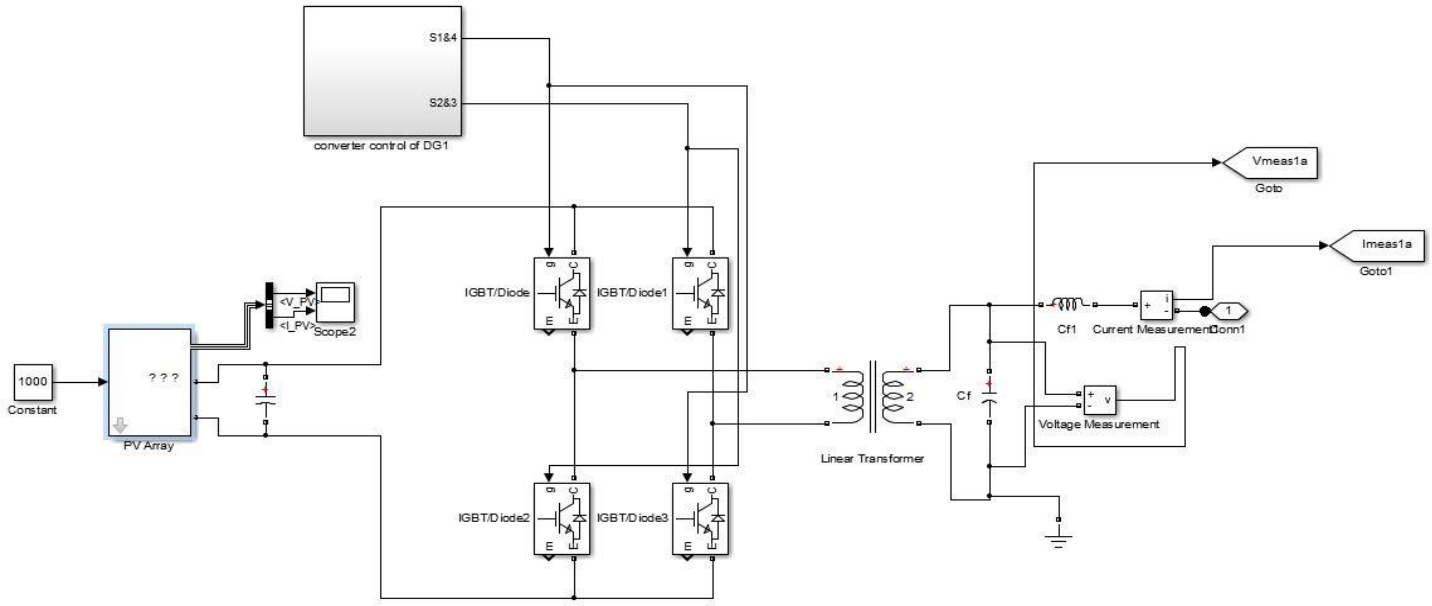

Fig.4b Converter structure of DG-1 with PV array

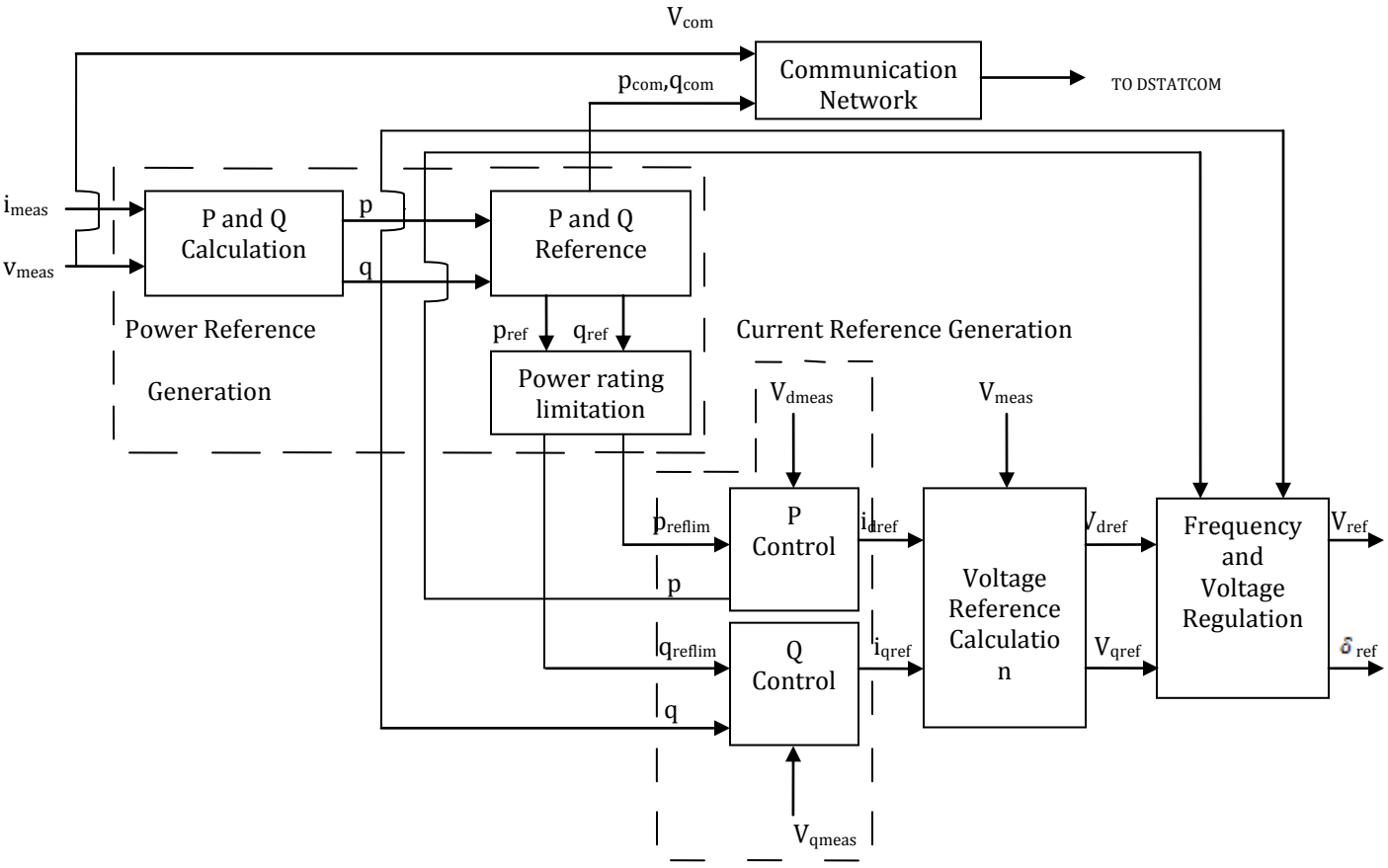

Fig. 5 Converter control scheme of DG-1

In the converter control of DG-1, the main blocks are the power reference generation, current reference generation and voltage reference generation. In power reference generation, real and reactive power generated based on the converter current limit and available power. The Real and reactive powers are limited to their respective real and reactive power limits. In the current reference generation, the current reference is generated from reference power and measured power. The error in the real power is used to calculate the d axis current reference by using p controller while the error in reactive power is used to calculate the q axis current reference by using q controller. In the voltage reference generation, current errors are passed through PI controller and added to get the d axis and the q axis voltage references. Important point to be considered is that in the islanded mode of operation only, the frequency and the voltage regulation are active and not in the other modes.

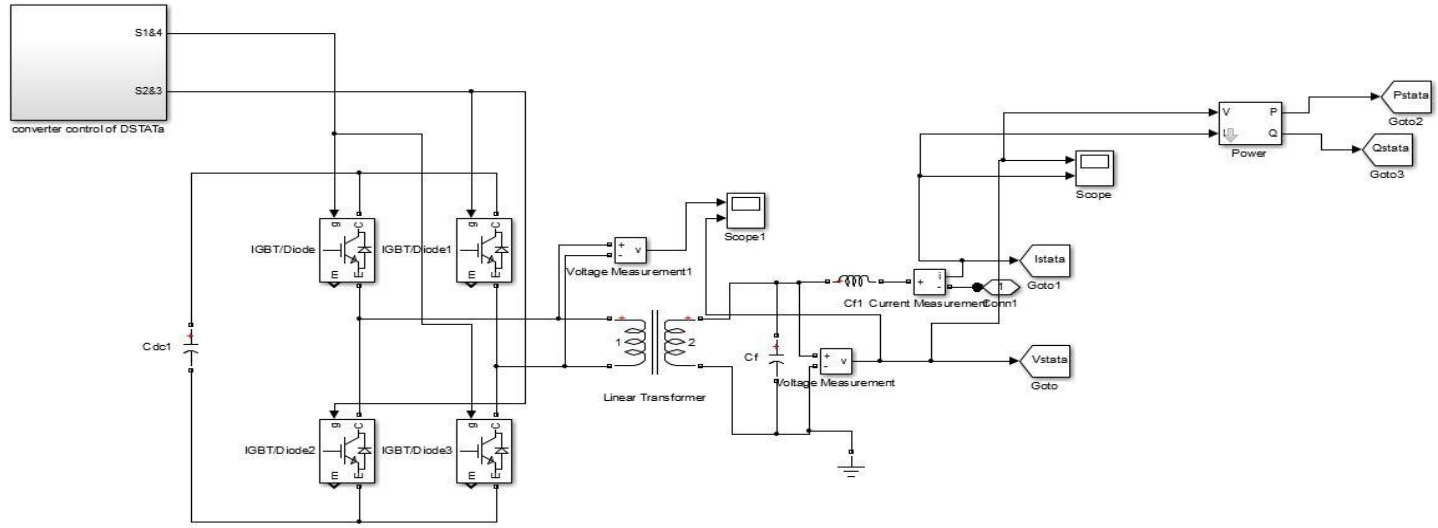

Fig. 6a Converter structure of DSTATCOM without PV array

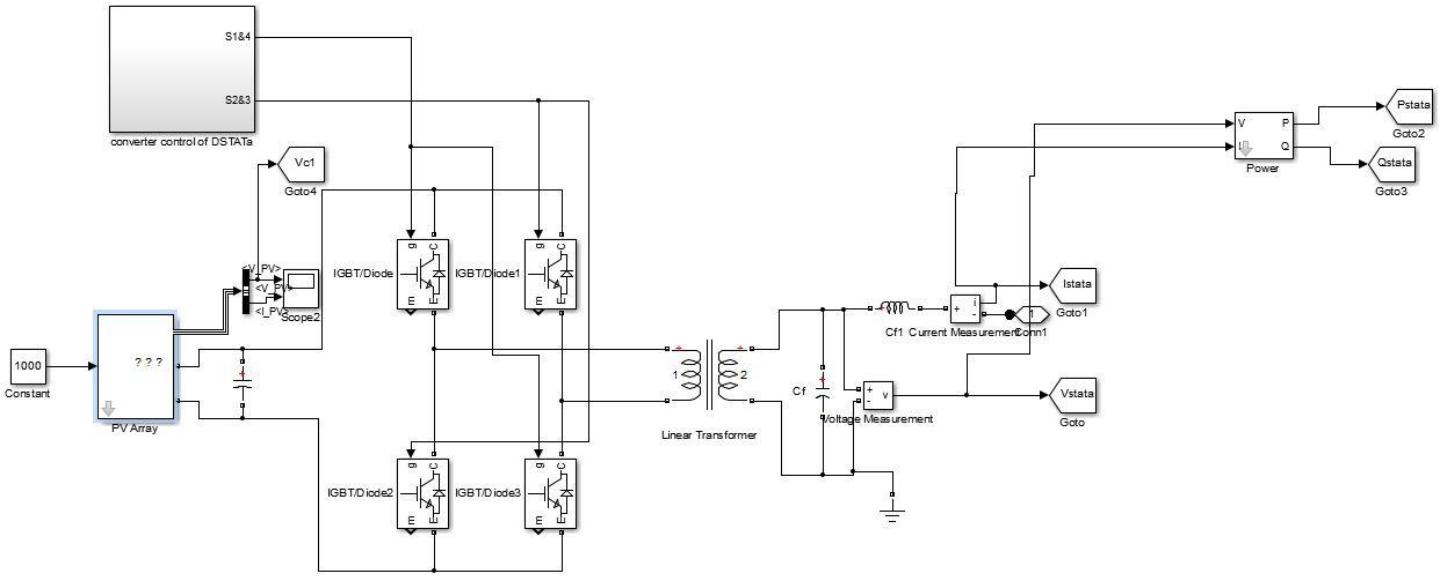

Fig. 6b Converter structure of DSTATCOM with PV array

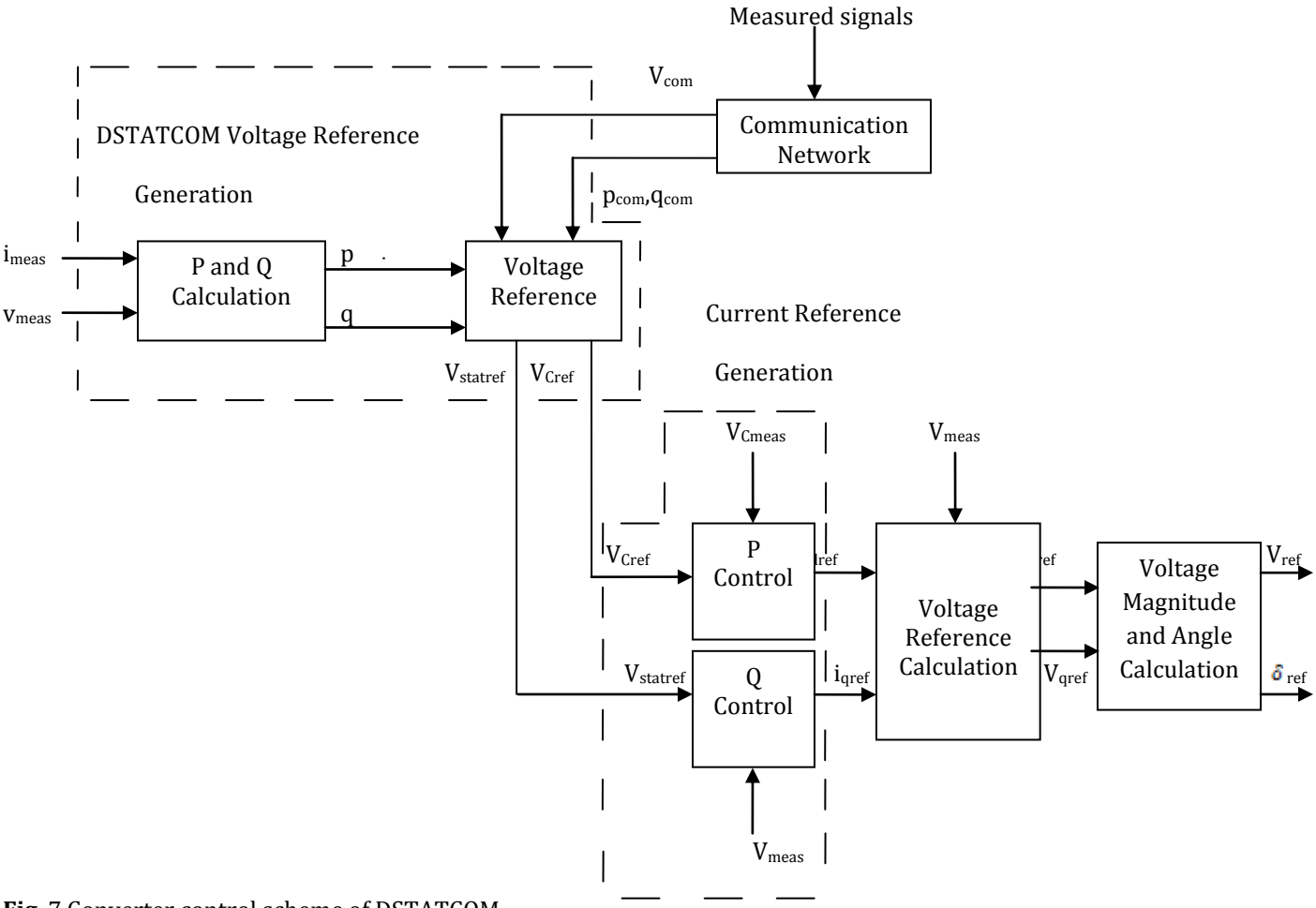

Fig. 7 Converter control scheme of DSTATCOM

In converter control of DSATATCOM, its output voltage reference $V_{statref}$ is calculated by the equation (9) and its dc voltage is fixed to a value of V_{cref}. In current reference generation, the error in dc capacitor voltage is passed through PI controller which generates the d axis current reference and error in DSTATCOM output voltage generates the q axis current reference. These current references and measured voltage are helpful in calculation d and q axis voltage reference calculation and these further helps in calculation of voltage magnitude and angle.

5. SIMULATION OF TEST SYSTEM

Fig. 1 is the test system simulated for various cases of no reactive compensation, reactive compensation on local measurement, and reactive compensation with operation of DG and DSTATCOM, Communication node failure at DG, Communication node failure at DSTATCOM.

To test performance, three sequences phenomenon sequence 1(grid connected mode operation), sequence 2(autonomous operation), sequence 3(grid connected followed by islanding) used. Simulation layout is as shown in Fig. 9

Consideration of similar set of change in DG power output and load switching sequence done for the purpose of comparison of controller performance for all the cases.

Sq-1: Assumption that system operation is in utility-connected mode is made. System running in steady state, all DGs supplying rated power and all loads are connected, 3 DGs power outputs are connected to phase A for which each ones limit is 2 kW. Limitation of 300 VAr for reactive powers is done.

Sq2: Assumption that system operation is in islanded mode is made. System running in steady state, all DGs supplying rated power and all loads are connected, 3 DGs

power outputs connected at Bus 2 of all 3 phases for which each ones limit is 2 kW. Limitation of 400 VAr for reactive power is done.

Sq3: Assumption that system operation is in utility-connected mode is made. When system running in steady state, all DGs supplying rated power and all loads are connected, at 0.8 sec microgrid is islanded. Load demand supplied by the DGs. 3 DGs power outputs connected at Bus 2 of all 3 phases for which each ones limit is taken as 2 kW at 1.1 sec. At 2.0 sec, loads connected at Bus 1 of phases A and B are disconnected to reduce the power demand in microgrid.

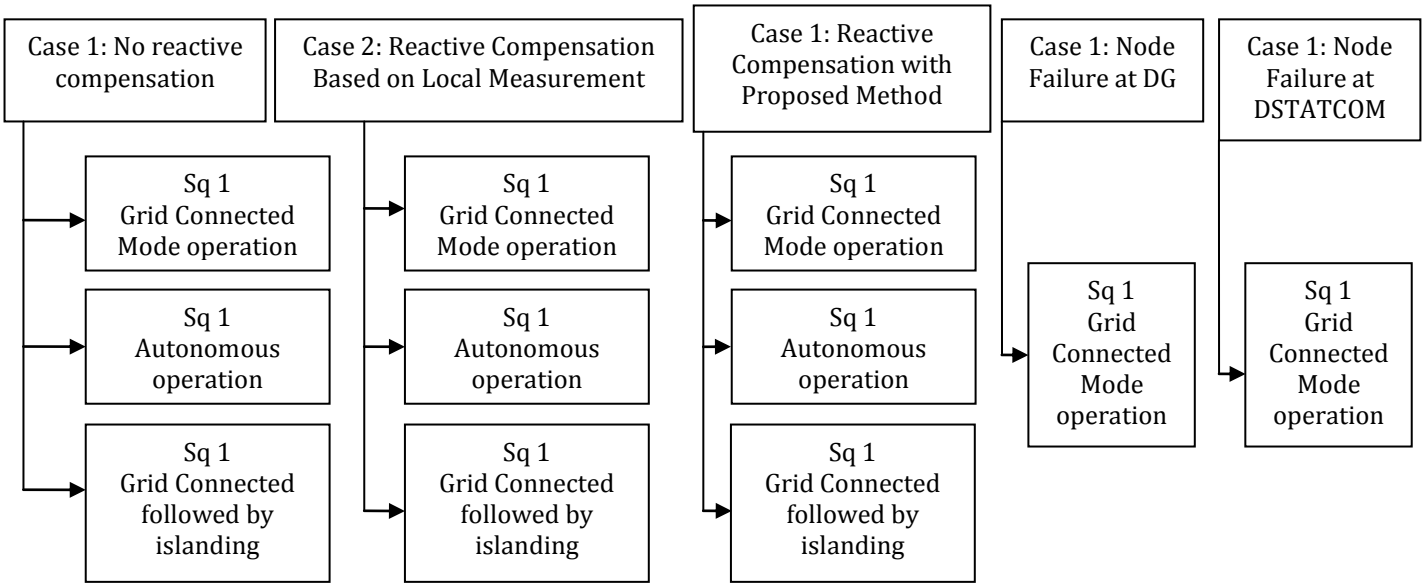

Fig. 9 Simulation Layout

6. RESULTS AND ANALYSIS

WITHOUT PV ARRAY:

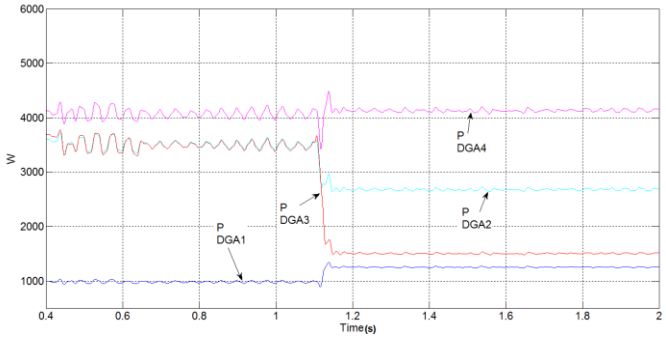

Fig. 10 Power output of the DGs in phase A

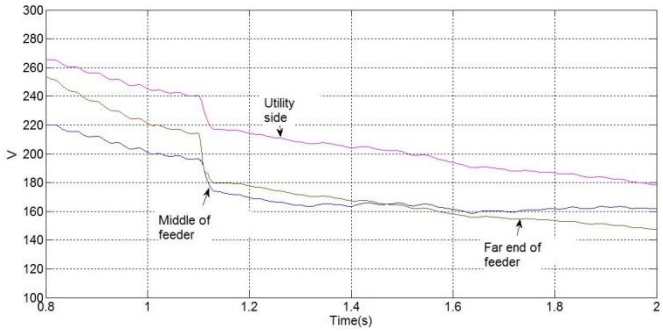

Fig. 11a RMS Voltages at phase A

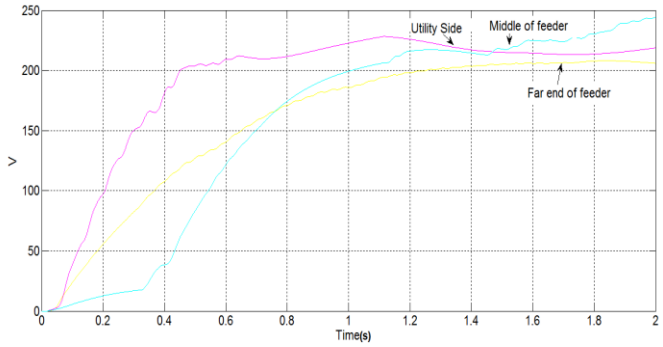

Fig. 11b RMS Voltages at phase B

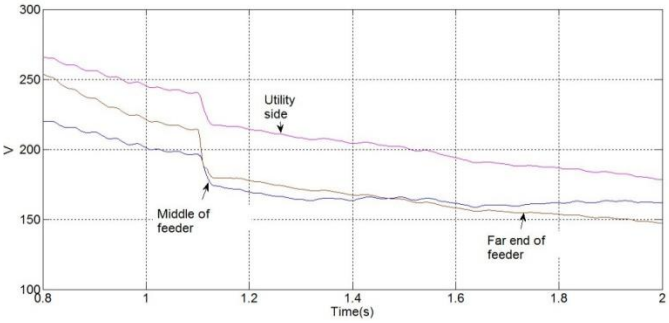

Fig. 11c RMS Voltages at phase C

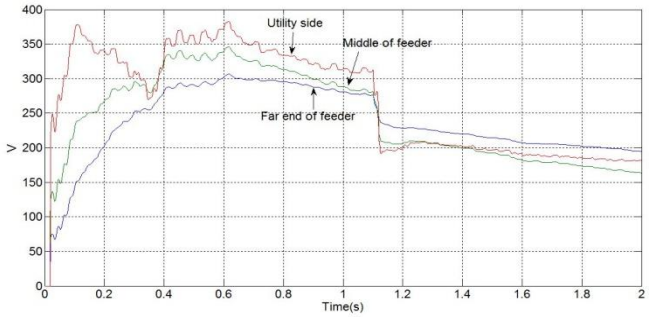

Fig. 12a RMS Voltages at phase A in Sq-2

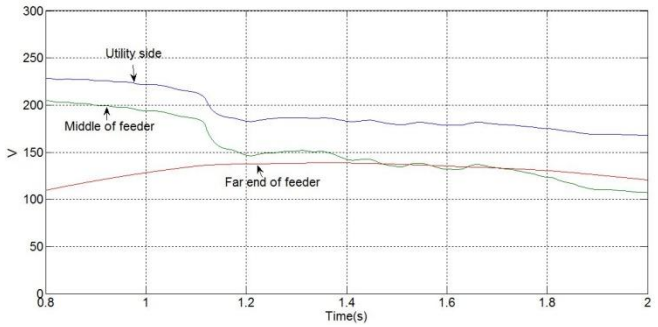

Fig. 12b RMS Voltages at phase B in Sq-3

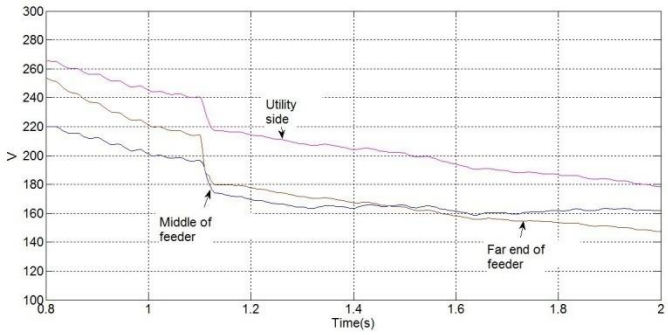

Fig. 13 RMS Voltages of phase A in Sq-1 with D-STATCOM

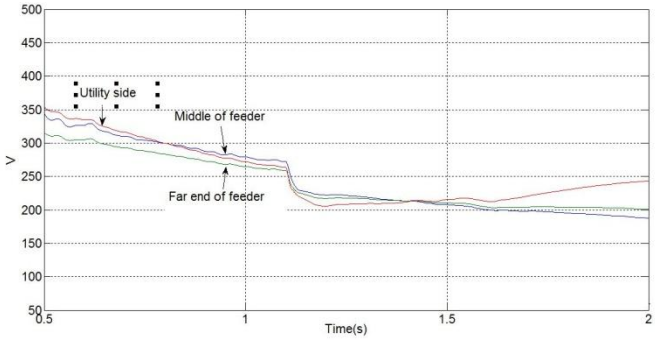

Fig. 14a RMS Voltage of phase A in different location

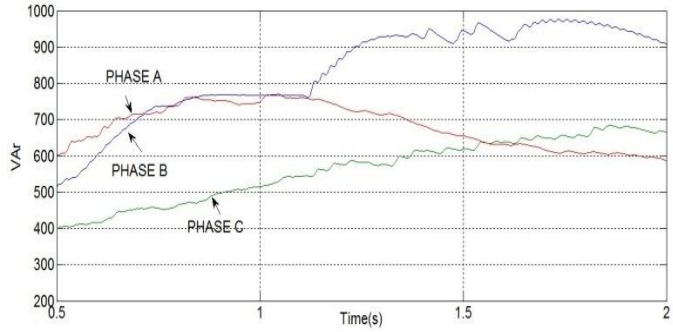

Fig. 14b Reactive power injected by DSTATCOM in three different phases

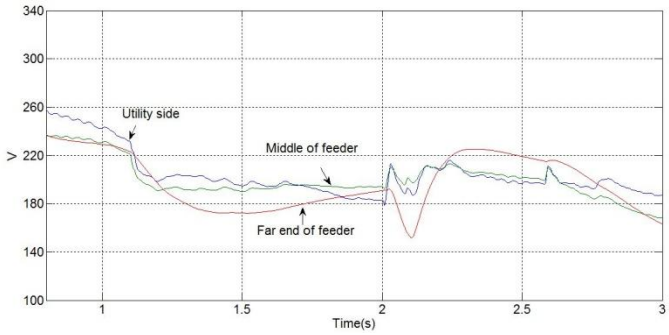

Fig. 15a RMS Voltages of phase A in Sq-3

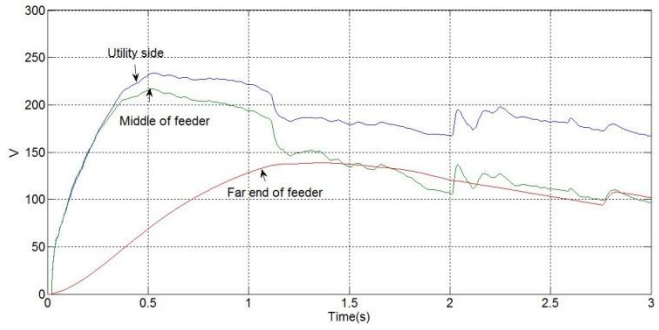

Fig. 15b RMS Voltages of phase B in Sq-3

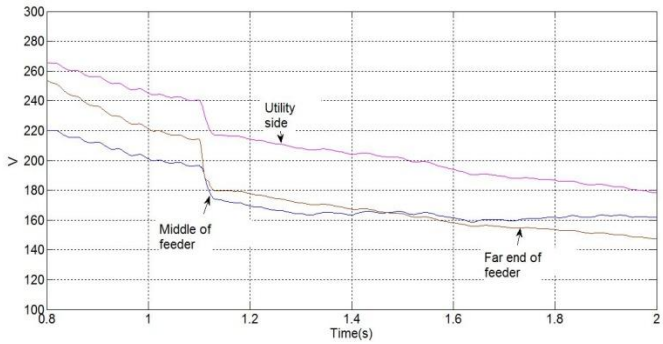

Fig. 16a RMS Voltages phase A in Sq-1 with proposed method

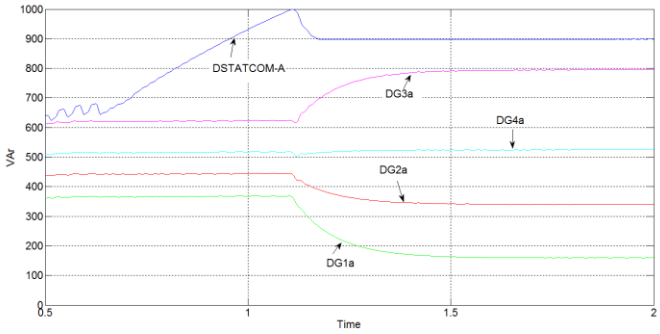

Fig. 16b Reactive power injection of DSTATCOM and DGs

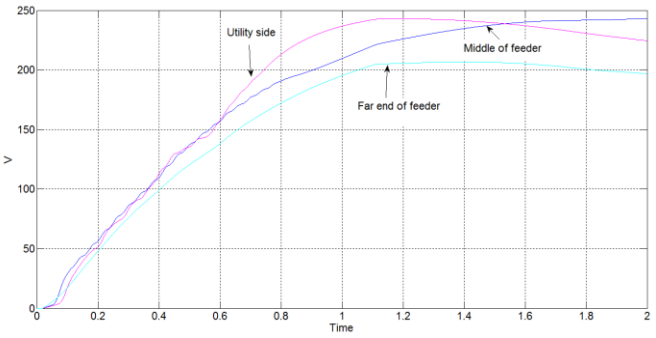

Fig. 17a RMS Voltages in phase A in Sq-2

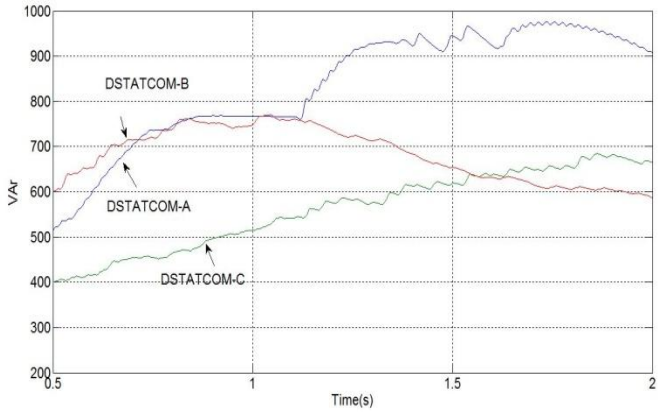

Fig. 17b Reactive power injection of DSTATCOM in three phases

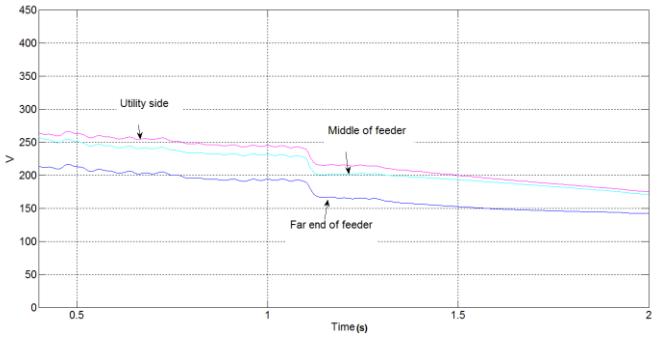

Fig. 20 RMS Voltages of phase A in Sq-1 followed by a DSTATCOM node failure

WITH PV ARRAY:

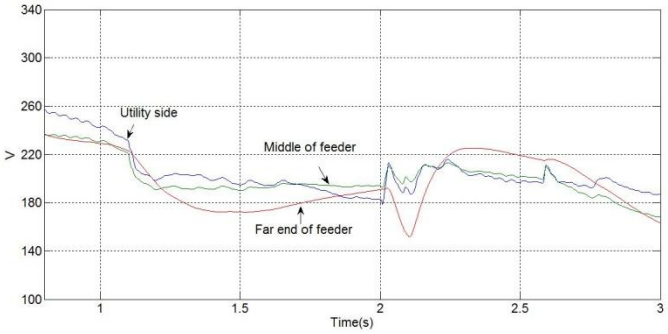

Fig. 18 RMS Voltages of phase A in Sq-3

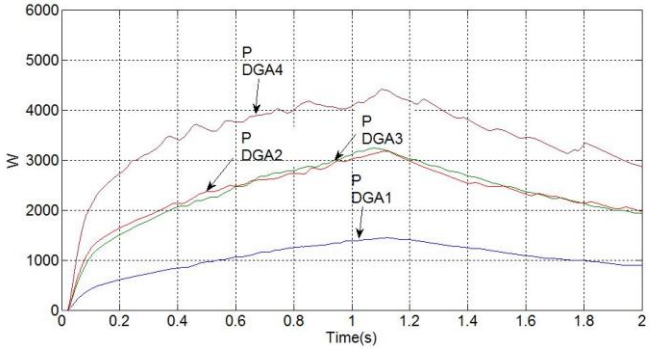

Fig. 21 Power output of the DGs in phase A

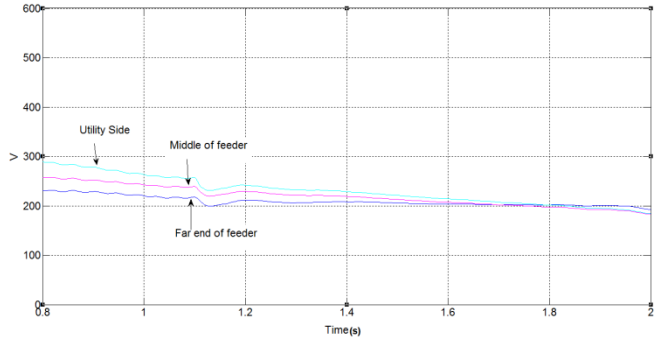

Fig. 19 RMS Voltages of phase A in Sq-1 followed by a DG node failure

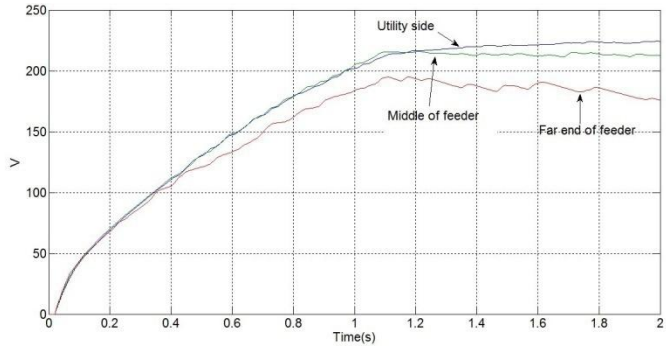

Fig. 22a RMS Voltages at phase A

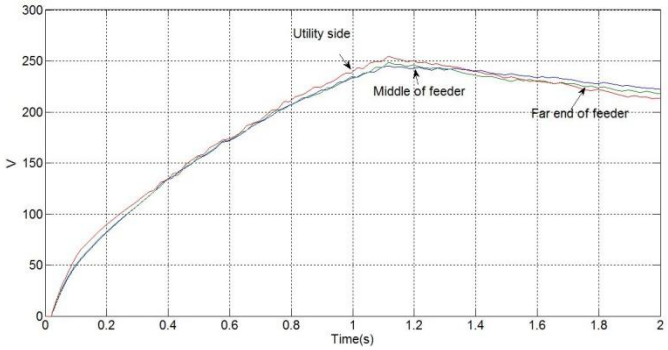

Fig. 22b RMS Voltages at phase B

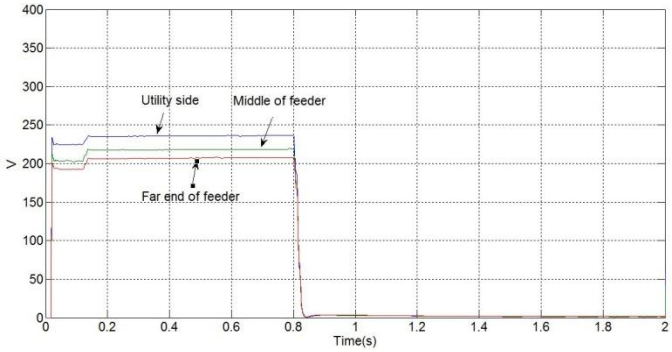

Fig. 23b RMS Voltages at phase B in Sq-3

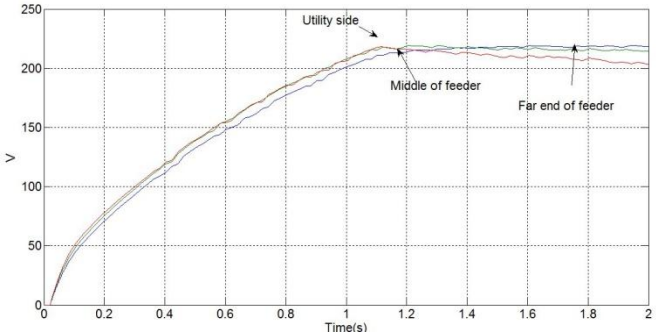

Fig. 22c RMS Voltages at phase C

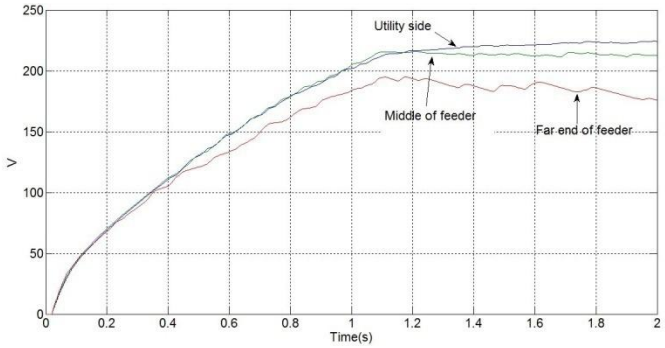

Fig. 24 RMS Voltages of phase A in Sq-1 with D-STATCOM

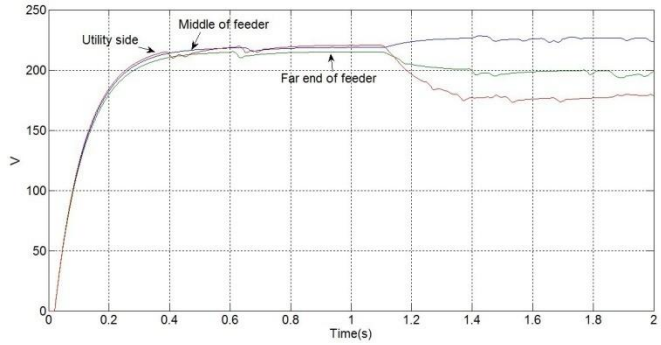

Fig. 23a RMS Voltages at phase A in Sq-2

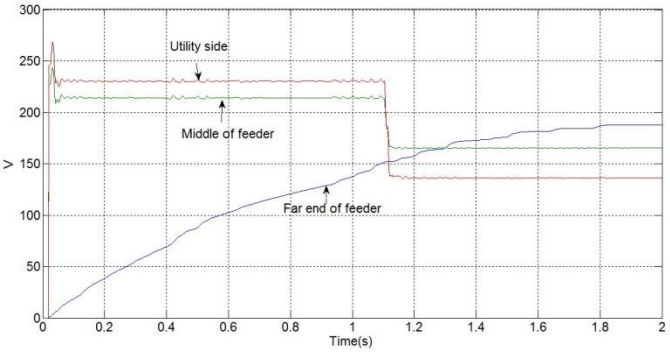

Fig. 25a RMS Voltage of phase A in different location

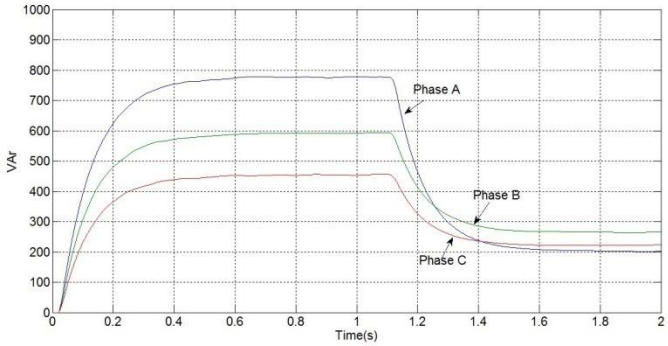

Fig. 25b Reactive power injected by DSTATCOM in three different phases

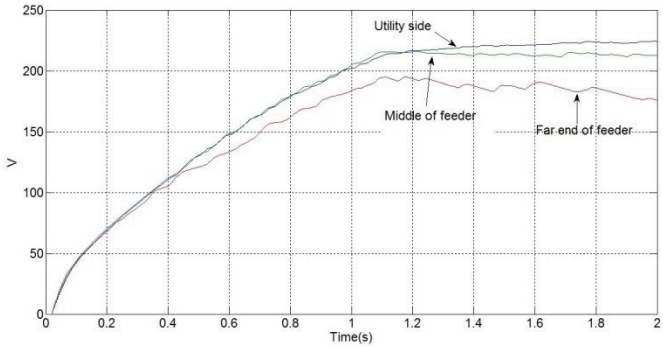

Fig. 27a RMS Voltages phase A in Sq-1 with proposed method

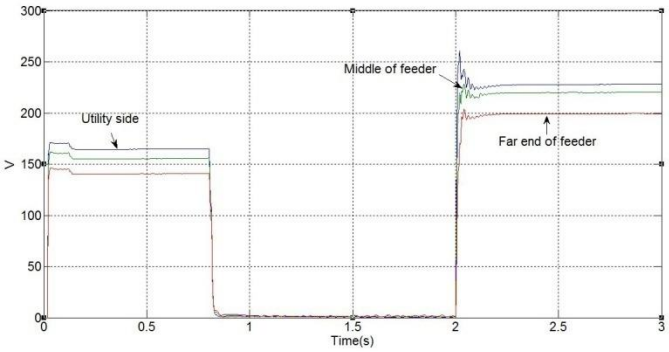

Fig. 26a RMS Voltages of phase A in Sq-3

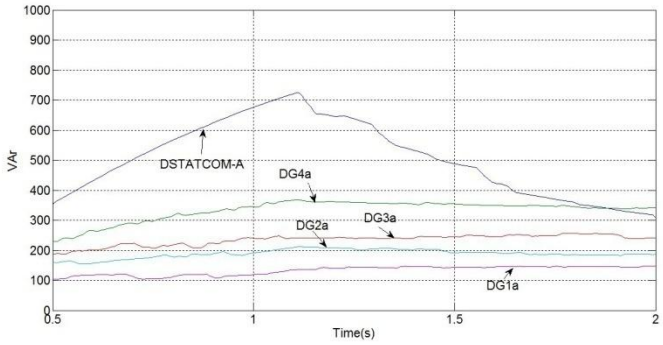

Fig. 27b Reactive power injection of DSTATCOM and DGs

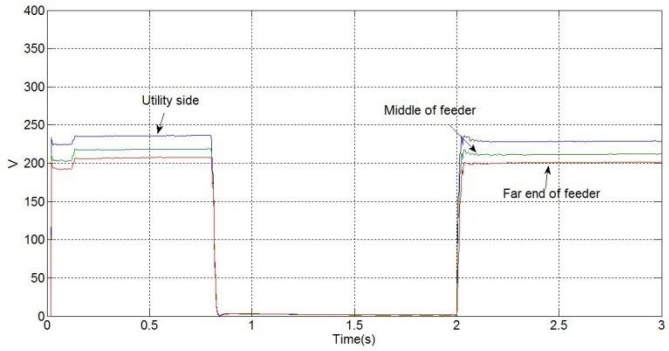

Fig. 26b RMS Voltages of phase B in Sq-3

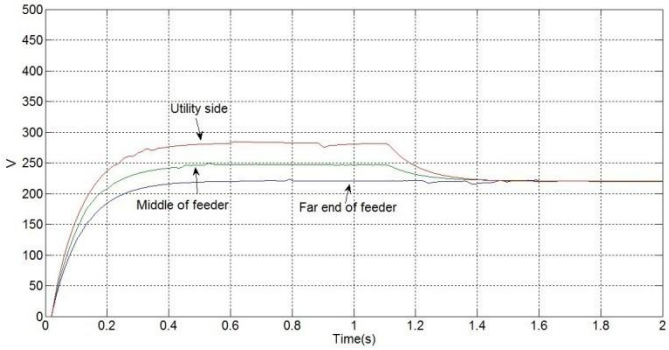

Fig. 28a RMS Voltages in phase A in Sq-2

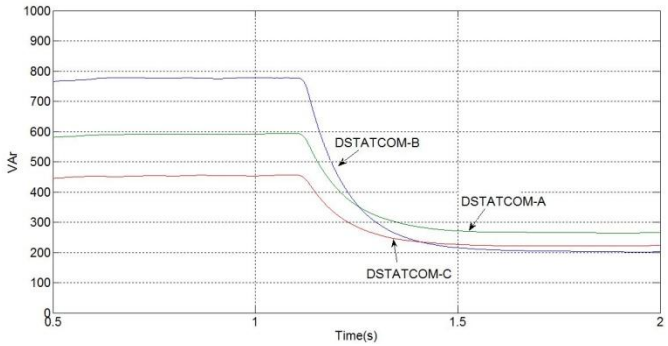

Fig. 28b Reactive power injection of DSTATCOM in three phases

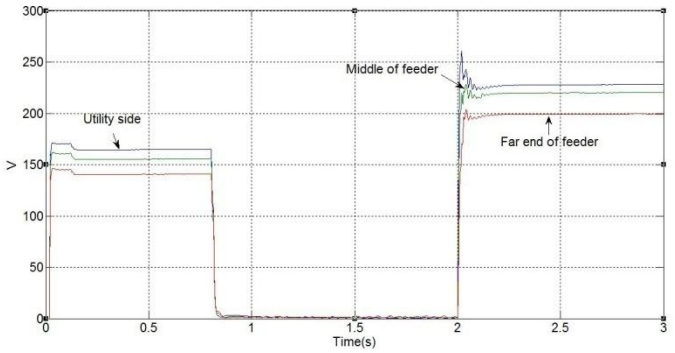

Fig. 29 RMS Voltages of phase A in Sq-3

A. Case 1: No Reactive Compensation

Reactive compensation not considered in this case and the DGs supplied total reactive power and utility in the grid-connected mode and in autonomous mode only by the DGs. For Sq-1, the power output of the DGs connected to phase A is shown in Fig. 10 and 21, while the voltage profile in three phases is shown in Fig. 11 and 22. It can be seen that in the far end and middle of the feeders, voltage regulation problem is more. In utility-connected side, voltage sag remains within 2%. The voltage unbalance and RMS voltage for Sq-2 and Sq-3 are shown in Fig. 12 and 23. It can be seen that the voltage regulation problems exist and the voltage drop is far more than the acceptable values.

B. Case: Reactive Compensation on Local Measurement

DSTATCOM works in a conventional way in this case. Depending upon the local bus voltage of the DSTATCOM, the reactive power injection takes place. The RMS voltage for Sq-1 is shown in Fig. 13 and 24. The reactive power injections by the DSTATCOMs and RMS voltages in Sq-2 and Sq-3 are shown in Figs. 14, 25 and 15, 26 respectively. It can be seen that in comparison to the case where no compensation is used, voltage profile is improved in this case. Though voltages are below limit is some cases, reactive power compensation works well only close to DSTATCOM.

C. Case 3: Reactive Compensation with Proposed Method

The reactive compensation is achieved with proposed method given by the equation from (9)–(11) in which with the help of local bus voltage and power flow in the line, DSTATCOM reactive compensation modulated and depending upon voltage sag, active power injections of DGs are modulated to increase the reactive power injection limit.

The RMS voltages of phase A in Sq-1 are shown in Fig. 16a and 27a. The voltage profile improves within 10% tolerance. Fig. 16b and 27b shows the reactive power injection by the DSTAT-a and DGs connected to A phase. The change of reactive power in DG3a and DG4a validates (10).

The system response in Sq-2 with the proposed controller is shown in Fig. 17 and 28. Phase A voltage and reactive power injection from different DSTATCOM shows system operation in efficient and stable manner.

In Sq-3, the voltages in phase A are shown in Fig. 18 and 29. Because of the proposed method, compensation is achieved and voltages kept within acceptable range.

D. Case 4: Communication Node Failure at DG

Assumption of communication node failure at DG-1a is made in this case., The system operates in Sq-1 with proposed control method. The system response is shown in Fig. 19. With DG power limit as described in Sq-1, phase A voltage changes at 1.1 sec. At 1.75 sec, node failure simulated, and the utility side voltage falls. No visible changes experienced in voltages at the middle and far end of the feeder.

E. Case 5: Communication Node Failure at DSTATCOM

Consideration of communication node failure at DSTATCOM is made in this case. The system response for a node failure at DSTAT-a is shown in Fig. 20 Assumption that system operates with proposed controller in Sq-1 and

at 1.1 sec, DG power is limited as described in Sq-1. At 1.75 sec, node failure simulated, and voltages dropped in utility side, middle, and far end of the feeder. DSTAT-a operates with local measurements similar to Case 2 in this case. However, in comparison to case 2, improvement in voltages resulted due to modulating the DG active power as (10)

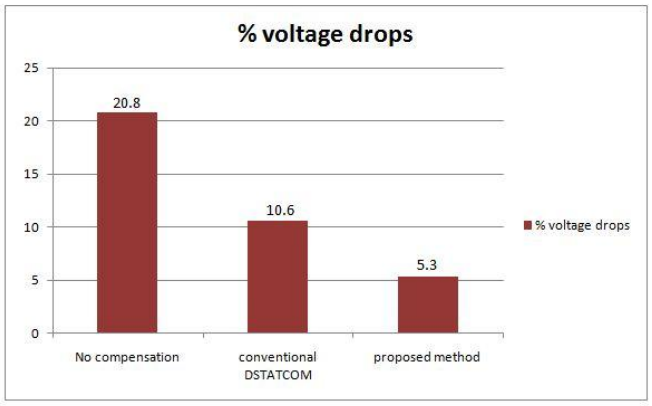

Fig. 30 Average voltage drop without PV array

TABLE V

PHASE A RMS VOLTAGE FROM SIMULATION RESULTS WITHOUT PV ARRAY

Seq&fig.No	Initial value(V)	In step1	In step2	Final Value
Seq.1-Fig11(a) Grid connected	U.S=220 MF=215 FE=203	---	---	U.S=208 MF=182 FE=180
Seq.2-Fig12(a) autonomous	U.S=310 MF=290 FE=280	---	---	U.S=220 MF=205 FE=190
Seq.1-Fig13 Grid connected	U.S=221 MF=214 FE=200	---	---	U.S=182 MF=175 FE=165
Seq.2-Fig14(a) autonomous	U.S=275 MF=268 FE=260	---	---	U.S=230 MF=210 FE=200
Seq.3-Fig15(a) islanding	U.S=230 MF=225	U.S=218 MF=216	U.S=216 MF=213	U.S=229 MF=218

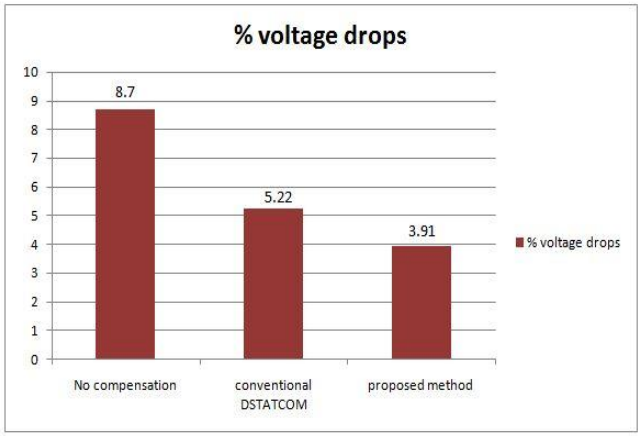

Fig. 31 Average voltage drop with PV array

TABLE VI

PHASE A RMS VOLTAGE FROM SIMULATION RESULTS WITH PV ARRAY

Seq&fig.No	Initial value(V)	In step1	In step2	Final Value
Seq.1-Fig11(a) Grid connected	U.S=200 MF=208 FE=203	---	---	U.S=225 MF=210 FE=190
Seq.2-Fig12(a) autonomous	U.S=220 MF=204 FE=192	---	---	U.S=223 MF=218 FE=197
Seq.1-Fig13 Grid connected	U.S=221 MF=214 FE=200	---	---	U.S=220 MF=193 FE=186
Seq.2-Fig14(a) autonomous	U.S=226 MF=212 FE=210	---	---	U.S=228 MF=214 FE=206
Seq.3-Fig15(a) islanding	U.S=227 MF=218	U.S=220 MF=213	U.S=219 MF=210	U.S=229 MF=221

Comparison of the controllers performance:

From simulation results, proposed controller ensures acceptable voltage regulation in all cases. Performances in various operating modes are compared as follows:

•Without any reactive compensation, voltage goes below acceptable limit in grid-connected mode [Case 1, Fig. 11a and 22a]. Depending upon local measurement, reactive compensation (Case 2, Fig. 13 and 24) results in improvement of voltage profile, but at the far end of the feeder, voltage regulation is not good. Proper reactive compensation provided by the proposed controller and voltage kept within acceptable value [Case 3, Fig. 16a and 27a].

•Without any compensation, voltage goes below regulation limit in autonomous mode [Case 1, Fig. 12a and 23a].
while depending upon local measurement, reactive compensation results in improvement of voltage profile [Case 2, Fig. 14a and 25a]. The proposed controller further results in improvement of voltage profile [Case 3, Fig. 17a and 28a].

•Performance wise the proposed controller in islanding sequence (case 3, Fig. 18 and 29) is much better than local reactive compensation in case 2 [Fig. 15a and 26a]. In this autonomous operation case, improvement of voltage by proposed controller takes place significantly.

•At utility side of DG communication node failure, the impact is very less (Case 4, Fig. 19) as other DGs continue to communicate with DSTATCOM.

•DSTATCOM communication node failure has a larger impact (Case 5, Fig. 20) because of all communications to DSTATCOM ceased. Without communication to DSTATCOM is similar to Case 2 with local measurement only. However, a little difference is created due to DG adaptation of reactive limit works properly.

Different cases are simulated with the proposed method, and the average voltage drop stays within limit in all the cases. The average voltage drop without compensation, with conventional DSTATCOM, and with the proposed method is shown in Fig. 30 and 31 without and with PV array.

Table V and VI gives the initial, intermediate and final steady-state values of phase A without and with PV array.

7. APPENDIX

Tables I, II, III, IV gives the data for grid and load in the microgrid, converter and controller, DG controller gains and DSTATCOM gains.

8. CONCLUSION

In this project, a new control technique for single-phase DSTATCOM with DG is presented. The application is aimed for microgrid feeding single-phase loads with feeders spanned geographically far apart covering small communities. This reactive power compensation is based on local measurement as well as the power flow in the lines. It is shown that the proposed method reduces the voltage drop more effectively while maintaining the voltage regulation with a high penetration of the DGs. The simulation of test system validates the DSTATCOM superior performances under different operating conditions. The results are analyzed with the extension of using the solar energy system for checking the real time performance of the system given. And the results are achieved as per the ideal simulations in practical solar system also.

REFERENCES

[1] R.Majumder, “Reactive power compensation in single phase operation of microgrid,” *IEEE Trans. Ind. Electron.*, vol. 60, no. 4, pp. 1403 -1416, Apr. 2013.

[2] X.Yoasuo, C.Liuchen, B.K.Soren, B.Josep, and S.Toshihisa, “Topologies of single-phase inverters for small distributed power generators: An overview,” *IEEE Trans. Power Electron.*, vol. 19, no. 5, pp. 1305–1314, Sep. 2004.

[3] T.E.McDermott and R.C.Dugan, “Distributed generation impact on reliability and power quality indices,” in *Proc. IEEE Rural Elect. Power Conf.*, 2002, pp. D3_1–D3_7.

[4] National Energy Technology Laboratory, U.S. Department of Energy *Provides Power Quality for 21st Century Needs*, Jan. 2007.

[5] 978-1-84800-317-0 R.Strezelecki and G.Benysek, “Active power quality controllers,” in *Power Electronic in Smart Electrical Energy Network*. New York: Springer-Verlag, 2011.

[6] R.Majumder, A.Ghosh, G.Ledwich, and F.Zare, “Operation and control of single phase micro-sources in a utility connected grid,” in *Proc. IEEE PES*, Jul. 26–30, 2009, pp. 1–7.

BIOGRAPHIES

B.Praveena is currently pursuing her M.Tech degree in Electrical and Electronics Engineering with specialization in Electrical Power Systems from Jawaharlal Nehru Technological University, Anantapur, India. She did her B.Tech Degree in Electrical and Electronics Engineering from Intell Engineering College Anantapur,India 2013.

S.Sravanthi is currently pursuing her M.Tech degree in Electrical and Electronics Engineering with specialization in Electrical Power Systems from Jawaharlal Nehru Technological University, Anantapur, India. She did her B.Tech Degree in Electrical and Electronics Engineering from AudiShankara institute of technology Gudur,India 2012.